

Published in final edited form as:

J Electrocardiol. 2010 ; 43(6): 530–534. doi:10.1016/j.jelectrocard.2010.08.005.

Cardiac late potential signals and sources

Edward J. Berbari, PhD^{a,*} and Carolina Vasquez, PhD^b

^aIndiana University Purdue University Indianapolis, Indianapolis, IN, USA

^bNew York University School of Medicine, New York, NY, USA

Abstract

Most studies of cardiac late potentials (LPs) recorded from the body surface use signal processing definitions to characterize these abnormal ventricular potentials. For many years, the focus of the clinical studies have been on those signals that outlast the QRS complex; however, cardiac mapping studies have clearly identified that the such abnormal activation occurs during the QRS complex as well and can be distinguished from normal QRS potentials using advanced signal processing tools. Thus, both the abnormal intra-QRS potentials and the LP represent a continuum of the same signal sources. The electrogram recordings of these signals are often characterized as multiphasic with ambiguous/multiple depolarization times spanning tens of milliseconds within very short distances (<1.0 mm). The biophysical basis for these ambiguities does not fit conventional theories of cardiac propagation. This work examines the role that myofibroblasts (MFs) may play in facilitating conduction and producing very long conduction delays (10-30 milliseconds) between populations of close but isolated regions of normal cells. The prerequisite element of this hypothesis is that the MF can express gap junction proteins that align with the corresponding proteins in the myocardial cells. Membrane responsiveness studies of the MF did not detect, as expected, any ion channels capable of producing significant transmembrane currents or depolarizing potentials. However, in tissue-cultured preparations of neonatal mouse myocytes, a nonconducting gap (200-400 μm) was seeded with MF, and this gap was electrotonically bridged by the MF resulting in conduction velocities of 0.1 m/s. Such passive cell mediation of cardiac conduction would provide a biophysical explanation of LP as well as forming the basis of several hypothesized mechanisms of cardiac arrhythmias, such as microentry. A fiber model using a series of coupled Luo-Rudy cardiac cell models was interspersed with a simple resistor-capacitor model of the MF, which then demonstrated a range of conduction disorders including excessive delays (>30 milliseconds) and decremental conduction. Hence, the role of this passive cell coupling in the generation of abnormal patterns of conduction as well as arrhythmogenesis has yet to be fully determined but may in fact define another mechanism of cardiac conduction.

Keywords

Cardiac late potential; Myofibroblast; Cell coupling

Introduction

Disruptions in ventricular activation have been well recognized with both conduction system disorders as well as diseased regions within and surrounding infarcts, for example, peri-infarction blocks. These are quite readily recognized on the electrocardiogram (ECG) with

wide QRS complexes and significant QRS slurs and notches. However, experimental studies in animal infarct models and catheter-based mapping studies in humans have pointed out the fact that lower level signals are often present in confined areas of the ventricles. Often the signals from these delayed activation sites are not readily visible on the standard ECG, and there is a 30-year history of these so-called late potentials both based on mapping studies and signal-averaged ECG recordings. There is a significant literature on all of these topics, and the reader is referred them for more complete reviews.¹⁻³ Following are several introductory figures that illustrate the points for this article in a clear manor.

Fig. 1 shows an example of each recording technology demonstrating exceeding prolonged activation potentials from patients with normal duration QRS complexes. The top panel, from a patient presenting with recurring ventricular tachycardia, shows a standard ECG with a QRS duration of about 80 milliseconds. The left ventricular electrogram in the lower trace shows a low-level multiphasic recording outlasting the QRS complex by about 120 milliseconds. The bottom panel in this figure is the signal-averaged vector magnitude recording, also from a patient presenting with recurring ventricular tachycardia, obtained in the standard fashion. The QRS duration is about 100 milliseconds, and the late potential outlasts the QRS by about 180 milliseconds.

Fig. 2 shows a subset of in vitro unipolar electrogram recordings obtained from an epicardial tissue block from a 4-day-old canine infarct region with surrounding normal tissue and are spaced at 2 mm. The upper 2 rows show typical recordings from normal regions and are characterized by a single intrinsic deflection. The lower row of recordings overlays the infarct region and demonstrates significantly prolonged recordings, and each has several intrinsic deflections.

These figures provide evidence that very slow conduction can occur in relatively small regions of the heart. Traditional explanations for these observations have been that conduction occurs through very long and meandering pathways via viable cells within infarct regions. Within evolving infarct regions, some of these viable cells would have abnormal cellular action potentials with depressed upstrokes and therefore lead to slow conduction. Viable cells within healed infarct regions have been shown, however, to have normal action potential characteristics.⁴

The data depicted in Fig. 1 were not from patients with recent or evolving infarcts, and another explanation is required to explain such prolonged periods of ventricular activation. Another explanation is now offered that introduces a relatively new concept of cardiac conduction, which we will identify as passive cell facilitation. A recent group of studies have postulated that either endothelial cells or myofibroblasts (the focus of this study) can synthesize gap junction proteins, which can align with myocytes and become low resistive pathways and actually conduct the cardiac impulse without the need for depolarizable ion channels. Because these cells do not have any activation currents, they may only propagate the cardiac impulse via their passive electrical properties. These electrical properties are the gap junction resistance, the intracellular resistance, and the membrane capacitance. The latter 2 elements are directly dependent on the cell geometry. Hence, the mere existence of the gap junctions is a necessary but not sufficient condition for exhibiting passive cell facilitation. A review of the role of myofibroblasts was recently published by Rohr,⁵ which provides a strong rationale for these primary structural cells participating in arrhythmogenesis via the development of appropriate gap junction interconnections, even though they are electrically inexcitable as demonstrated by membrane responsiveness measurements.⁶

Two approaches were used in this study to establish the passive cell facilitation hypothesis. The first was to develop a tissue culture model whereby myocyte monolayers were seeded with myofibroblasts and were observed to reconnect 2 halves of the separated culture. In addition, electrical maps of these cultures demonstrated the synchronicity of the 2 halves albeit with significantly delayed propagation between the 2 halves. Several investigators have demonstrated these interconnections in culture.⁶⁻⁹ The second approach uses mathematical models of these cellular types along with appropriate connections and geometric considerations.¹⁰⁻¹³

Methods

There are 2 major thrusts in this article: the culturing of myocytes and myofibroblasts to produce a 2-dimensional model of conduction across an inexcitable gap and a mathematical model of myofibroblast inserts in a conducting myocyte fiber. The methods used in each are briefly summarized, and the reader is referred to Vasquez⁶ for a more detailed description.

The initial studies were aimed at characterizing the electrical properties of fibroblasts. As expected, membrane responsiveness studies demonstrated no identifiable excitation membrane currents. However, the actual conductance of the gap junctions, the intracellular resistance, and the actual membrane capacitance needed to be determined. Studies by Rook et al¹⁴ measured the gap junction conductivities of myocyte-fibroblast pairs in the range of 310 pS and 8 nS. A series of confocal microscopic studies were done to determine fibroblast volume and surface areas with average values of $4.4 \times 10^{-6} \mu\text{L}$ and $7.44 \times 10^{-5} \text{cm}^2$, respectively. Using typical values for specific capacitance of $1.0 \mu\text{F}/\text{cm}^2$ results in a membrane capacitance of 74.4 pF for these fibroblasts. Using an axial myoplasmic resistivity of $150 \Omega\text{-cm}$ results in a total axial resistance of 7.5 M Ω . The total series resistance of the 2 gap junctions and the axial resistance is approximately 500 M Ω . Hence, the working model for the fibroblast bridge is a resistor-capacitor circuit with a time constant of about 38 milliseconds.

For the typical cardiac cell, a Luo-Rudy (LRd) model¹⁵ was used in the fiber model. A series of 70 cells comprised the fiber with an insert of 1 to 4 fibroblasts or alternating sets of multiple inserts in the center of the fiber. For the model to be compared with our results in our tissue culture model, the cell length and radius of the LRd model were adjusted for the cultured neonatal mouse myocytes. These adjustments were made to maintain similar volume to surface area ratios as in the original model.

To compare results from the theoretical simulations to in vitro experiments, cell length and radius were adjusted from the LRd formulation (11- μm radius, 100- μm length) to the reported physical dimensions of cultured neonatal mouse cardiac cells, obtained by confocal microscopy methods.¹⁶ Myocyte and passive (fibroblast and endothelioid) cell radius was set to 4 μm . Cell length was fixed for myocytes and endothelioid cells at 32 μm . Fibroblast cell length varied from 28 to 38 μm . These parameters give volume to surface area ratios in the same order of the LRd model. Using a typical specific capacitance of $1 \mu\text{F}/\text{cm}^2$ gives cell capacitance values similar to those calculated from voltage clamp experiments on cultured neonatal mouse cardiac cells, as obtained from our cells and reported by Nuss and Marban.¹⁷ This approximation to a mouse myocyte is only in terms of cell size and gap junctional conductance. Mechanisms determining myocyte transmembrane currents remained under the LRd formulation

Isolated neonatal mouse ventricular cells were used in the tissue culture preparations. All monolayer preparations were done in special chamber (MEA 60 System; Multi Channel Systems, Reutlingen, Germany) with 60 surface electrodes embedded in the center of 5×5 -

cm glass substrate. The electrodes are made of gold-plated titanium nitride and placed in an 8×8 grid (minus the corners). The electrode diameter is $30 \mu\text{m}$, and the interelectrode distance is $200 \mu\text{m}$. The sampling data rate was 5000 Hz, and the recording bandwidth was 10 to 2000 Hz. After acquisition, the individual recording analysis and isochronous map creation were performed with a custom Matlab program developed in our laboratory. After 7 days, the tissue culture monolayer was divided by creating a gap to divide the monolayer in half. This was done by dragging a plastic micropipette tip through and across the center of the monolayer producing a gap of 200 to $600 \mu\text{m}$ wide. The scarred monolayers were then treated with 0.1 mM BrdU, which will slow the growth of fibroblasts and eliminate the growth of the endothelial cells.

Using the custom analysis program, the local activation time was initially determined by measuring the maximum dV/dt of the individual electrogram. Manual overreading can be performed to make adjustments. The program will do a local interpolation in the case of noisy or poor-quality recordings. Local conduction velocities can be calculated using spatial derivatives obtained with nearest neighbor recordings in the X or Y direction. Conduction velocity vectors and isochronal maps were generated for the scar models. Recoupling of the monolayer halves was determined by inspection of the recordings with sustained synchrony being the primary criterion.

Results

Fig. 3 shows a typical example of a map from the scarred monolayer “fused” by the growth of fibroblasts in the $350\text{-}\mu\text{m}$ -wide gap region. The isochronous map indicates a rapid activation (average velocity, 3.96 cm/s) until the gap region where conduction slows and ranged between 0.84 and 1.1 cm/s. The right half of Fig. 3 shows a micrograph of the gap region. The rectangular box encompasses 4 recording electrodes representing the left half monolayer, the gap region, and right half monolayer. The lower traces depict these 4 recordings. All of the recordings in the myocyte regions show a rapid biphasic recording typical of normal propagation. The second recording from the gap region shows 2 deflections labeled major and secondary. This is consistent with an electrotonic current flow.

Fig. 4 shows data from 4 variations of fibroblast inserts. Above each panel is a block sequence (shaded = myocyte [M], white = fibroblast [F]) depicting the specific inserts and repeating sequence. Panel A has an alternating single fibroblast insert. The resulting action potentials show a cumulative slowing of activation of 30 milliseconds spanning 6 alternating sets of FM inserts. Panel B also has six inserts but in an FFM pattern. Here the delay is more pronounced at 100 milliseconds. Panel C uses an FFFM pattern, and now the classic pattern of decremental conduction is observed. Finally, in panel D, the pattern is FFFF and complete block occurs.

Discussion and conclusion

The data presented in Figs. 1 and 2 clearly pointed to the need for developing a greater biophysical understanding of conduction in diseased regions of the heart. Once it was recognized that nonconducting cells could form gap junction interconnections with myocardial cells, then the line of discovery outlined in this article moved forward. Many others have also contributed to these underlying concepts, perhaps motivated more from the perspective of the basic biology involved. Our initial motivation drew its impetus from the clinical setting and the existing observations of cardiac late potentials obtained from both the electrophysiology laboratory-based catheter recordings and the body surface, high-resolution ECG recordings. Our laboratory undertook a major effort in cardiac mapping of canine infarcts to move closer to the source of these late potentials and generate a greater

understanding of their origin. However, ambiguous recordings from these regions, as shown in Fig. 2, did not provide us with any greater insight into the late potential sources, other than their actual existence and overall duration. Indeed, multiple depolarizations in a very small region only created greater confusion as to the nature of propagation within and surrounding the infarct regions.

This initial description of passive cell facilitation, in support of pathologically prolonged activation, has a number of limitations. These include the use of the LRd model, which was primarily derived from guinea pig data, whereas our cell culture observations used neonatal mouse cells. In addition, other numerical models of fibroblasts and forward models, which could have demonstrated extracellular recordings, were not included.

The passive cell facilitation hypothesis is a new model for abnormal cardiac conduction. Its actual presence in humans has yet to be confirmed. However, it appears to bring us closer to a greater understanding of the significantly prolonged depolarization potentials observed in both the clinical and experimental settings. Prolonged activation sequences in confined regions may be the result of other pathophysiologic substrates such as meandering pathways through fibrotic regions, which can be complex in a 3-dimensional volume. Concepts, such as microentry, have often been invoked to explain many observations. Passive cell facilitation provides a working biophysical model to actually move these concepts forward with the early evidence very encouraging in both the basic experimental setting and the use of mathematical modeling tools.

References

1. El-Sherif, N.; Turitto, G., editors. High resolution electrocardiography. Futura Publishing Company; Armonk (NY): 1992.
2. Gomes, JA., editor. Signal averaged electrocardiography. Kluwer Academic Publishers; Dordrecht: 1993.
3. Berbari, EJ.; Steinberg, JS. Futura Publishers; Armonk (NY): 2000. A practical guide to high resolution electrocardiography.
4. Ursell PC, Gardner PI, Albala A, Fenoglio JJ, Wit AL. Structural and electrophysiological changes in the epicardial border zone during infarct healing. *Circ Res*. 1985; 56:436. [PubMed: 3971515]
5. Rohr S. Myofibroblasts in diseased hearts: new players in cardiac arrhythmias? *Heart Rhythm*. 2009; 6:848. [PubMed: 19467515]
6. Vasquez, C. PhD Thesis. Purdue University; May. 2006 Biophysical basis of discontinuous propagation in the diseased myocardium.
7. Camelliti P, Green CR, Kohl P. Structural and functional coupling of cardiac myocytes and fibroblasts. *Adv Cardiol*. 2006; 42:132. [PubMed: 16646588]
8. Gaudesius G, Miragoli M, Thomas SP, Rohr S. Coupling of cardiac electrical activity over extended distances by fibroblasts of cardiac origin. *Circ Res*. 2003; 93:421. [PubMed: 12893743]
9. Chilton L, Giles WR, Smith GL. Evidence of intercellular coupling between co-cultured adult rabbit ventricular myocytes and myofibro-blasts. *J Physiol*. 2007; 583:225. [PubMed: 17569734]
10. Vásquez C, Siddiqui RA, Moreno AP, Berbari EJ. A fibroblast-myocyte model which accounts for slow conduction and fractionated electrograms in infarct border zones. *Comput Cardiol*. 2002; 29:245.
11. Vasquez C, Moreno AP, Berbari EJ. Modeling fibroblast mediated conduction in the ventricle. *Comput Cardiol*. 2004; 31:349.
12. Jacquemet V, Henriquez CS. Loading effect of fibroblast-myocyte coupling on resting potential, impulse propagation, and repolarization: insights from a microstructure model. *Am J Physiol Heart Circ Physiol*. 2008; 294:H2040. [PubMed: 18310514]
13. Sachse FB, Moreno AP, Abildskov JA. Electrophysiological modeling of fibroblasts and their interaction with myocytes. *Ann Biomed Eng*. 2008; 36:41. [PubMed: 17999190]

14. Rook MB, Van Ginneken ACG, De Longe B, et al. Differences in gap junction channels between cardiac myocytes, fibroblasts, and heterologous pairs. *Am J Physiol.* 1992; 263:C959. [PubMed: 1279981]
15. Luo CH, Rudy YA. dynamic model of the cardiac ventricular action potential. I. Simulations of ionic currents and concentration changes. *Circ Res.* 1994; 74:1071. [PubMed: 7514509]
16. Thomas SP, Bircher-Lehmann L, Thomas SA, Zhuang J, Saffitz JE, Kleber AG. Synthetic strands of neonatal mouse cardiac myocytes: structural and electrophysiological properties. *Circ Res.* 2000; 87:467. [PubMed: 10988238]
17. Nuss HB, Marban E. Electrophysiological properties of neonatal mouse cardiac myocytes in primary culture. *J Physiol.* 1994; 479(Pt 2):265. [PubMed: 7799226]

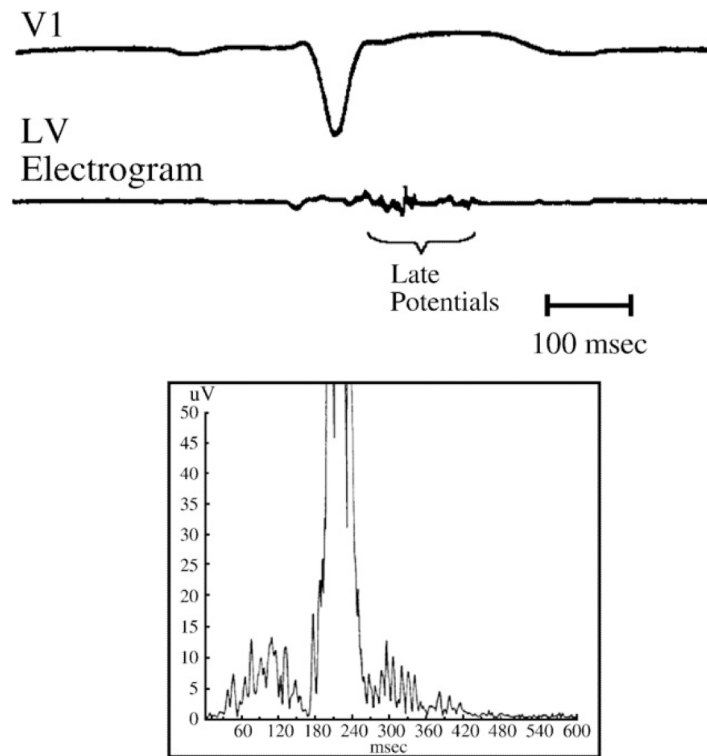


Fig. 1. Recordings demonstrating abnormally long depolarization potentials from patients with normal duration QRS complexes and no infarct. The top panel (courtesy of Dr Warren Jackman) shows lead V1 in the top trace and a catheter recording in the bottom trace. The electrogram recording outlasts the end of the QRS complex by 120 milliseconds. The lower panel is a signal averaged, filtered vector magnitude recording where the late potential extends to almost 180 milliseconds beyond the end of the QRS complex.



Fig. 2. Twelve unipolar electrograms obtained from a canine infarct model with a 2.0-mm spacing between recording sites. The epicardial region was excised and placed in a tissue bath. Each recording depicts 100 milliseconds. Note the multiphasic activity of the traces in the lower row of recordings indicating what appear to be closely timed and repetitive depolarizations.

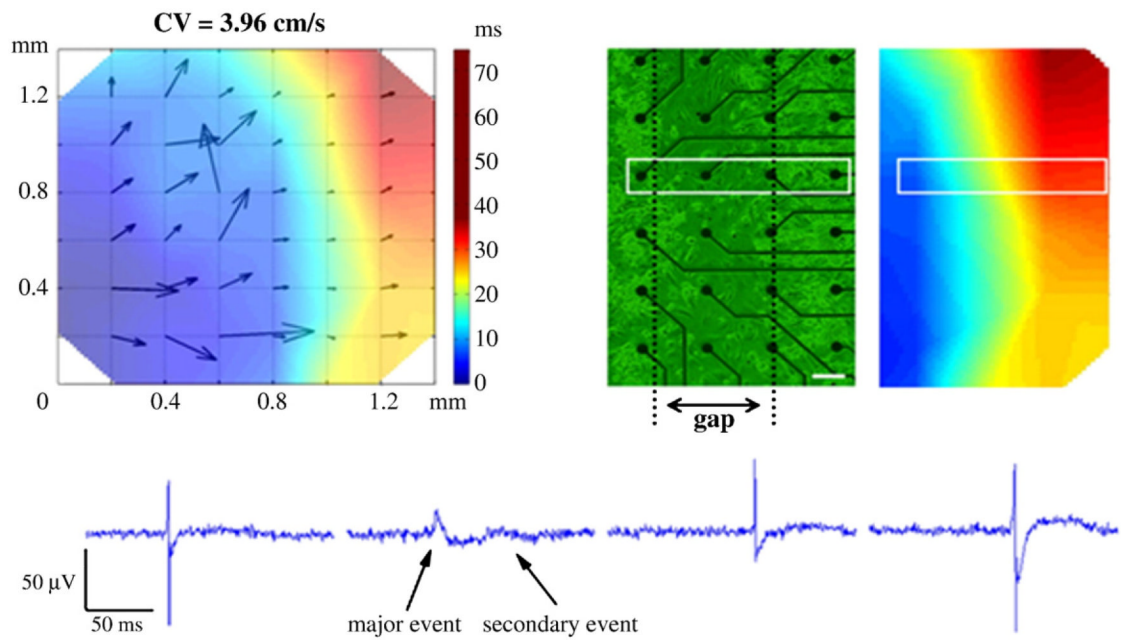


Fig. 3. Demonstration of conduction across the gap after fibroblast seeding. The upper left panel is an isochronous map demonstrating local conduction (arrows). The conduction slows to about 0.04 m/s across the gap as shown in the upper right panels. The lower traces depict electrogram recordings from the 4 electrodes depicted in the rectangle of the right panels.

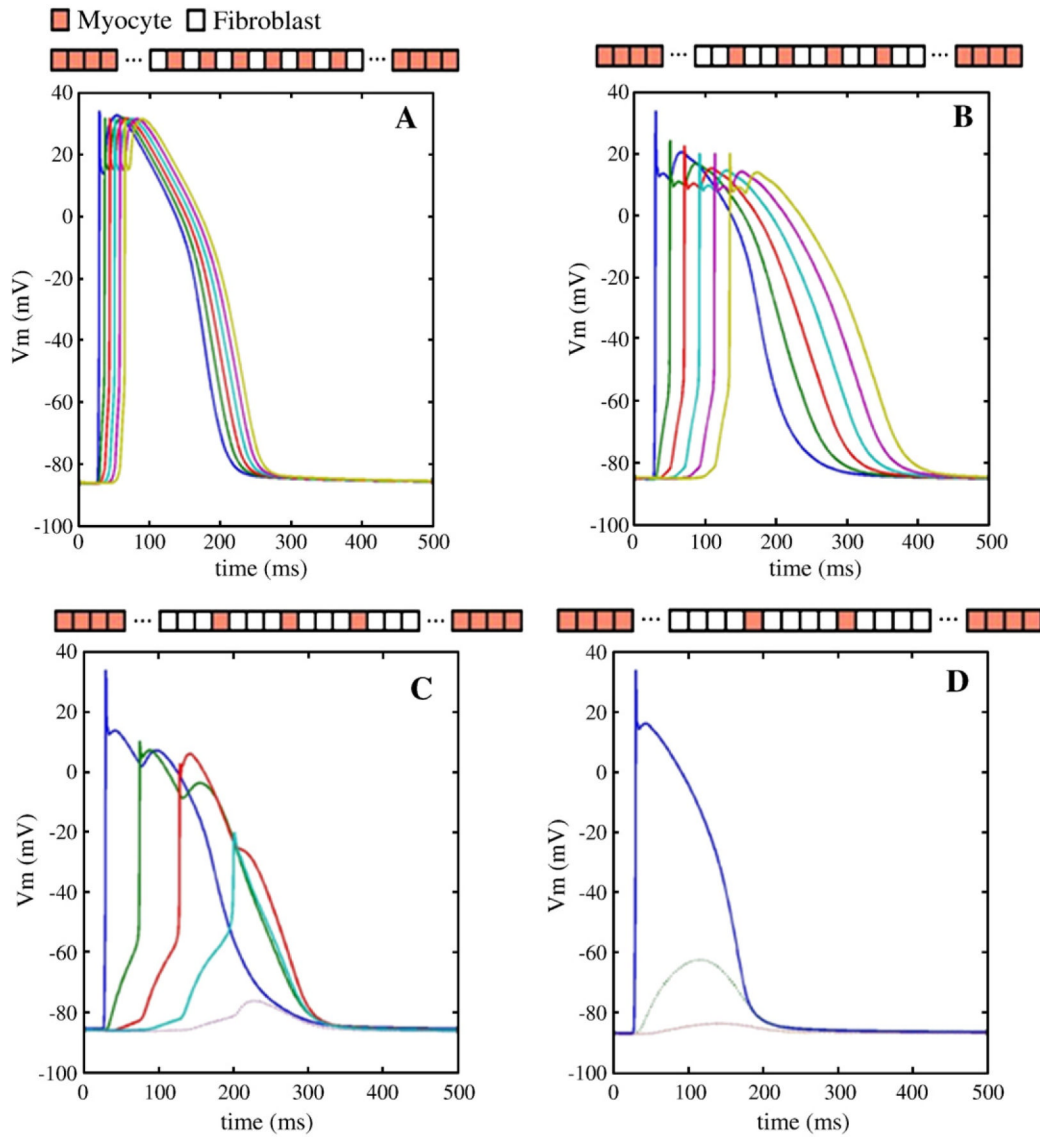


Fig. 4. Simulated action potentials from the myocyte fiber with fibroblast inserts. (A-D), Inserts of 1 to 4 fibroblasts as depicted in the white/shaded block sequences above each panel. (A and B), Propagation delays of 30 milliseconds and 100 milliseconds, respectively. (C), Decremental conduction. (D), Conduction block. Above each panel is a schematic block sequences showing the patterned relationship between myocytes and fibroblasts. It does not depict the actual scale.